RSC Advances

PAPER

View Article Online
View Journal | View Issue

Cite this: *RSC Adv.*, 2020, **10**, 19534

Discovery of hydrazide-based pyridazino[4,5-*b*] indole scaffold as a new phosphoinositide 3-kinase (PI3K) inhibitor for breast cancer therapy†

Ahmed A. M. Sarhan, *[a] Ahmed T. A. Boraei, [b] Assem Barakat [cd] and Mohamed S. Nafie ‡*[b]

Received 26th March 2020
Accepted 28th April 2020

DOI: 10.1039/d0ra02798g

rsc.li/rsc-advances

Herein, the mono and dialkylation of pyridazino[4,5-*b*]indole were achieved with a set of alkylating agents, including amyl bromide, allyl bromide, benzyl bromide and ethyl chloroacetate in the presence of K_2CO_3/acetone or KOH/DMSO. The hydrazinolysis of mono and di-esters **10** and **11** gave the target hydrazides **12** and **13**, which displayed promising, potent, and significant cytotoxic activity against the MCF-7 cell line with IC_{50} values of 4.25 and 5.35 μm compared to that of the standard drug 5-FU (IC_{50} 6.98 μm), respectively. RT-PCR analysis of the most active compound **12** was performed to determine its mode of action through the up-regulation of pro-apoptotic genes and inhibition of anti-apoptotic and PI3K/AKT/mTOR genes. The findings were consistent with the proposed mechanism illustrated in the *in silico* study. Further, the *in vivo* analysis exhibited its potent anti-cancer activity through the prolongation of survival parameters, and inhibition of ascetic fluid parameters in EAC-bearing mice.

1. Introduction

Targeted drug therapy for cancer treatment is one of the most important challenges in the new era because traditional cancer treatments have adverse side effects and drug resistance problems, resulting in the urgent need for safer, more effective targeted drug therapies with less side effects, which from an economical point of view is still a major challenge.[1]

One of the targeted receptors that play a significant role in cancer treatment is phosphatidylinositol 3-kinase (PI3K),[2] which is a lipid kinase and plays a crucial role in the signaling pathway of the PI3K/AKT/mTOR genes.[3,4] In diseases such as cancer and diabetes, the PI3K pathway has a high impact on the cell growth of cancer, motility, survival and metabolism. Thus, the design and development of drugs that may work as an inhibitor of PI3K singling in tumor therapy are highly interesting. Pyridazino[4,5-*b*]indol-4-ones and its analogues display significance in cancer therapy *via* the inhibition of DYRK1A[5] and PI3Kα in various human cancer cell lines.[6] Additionally, this interesting scaffold has been discovered to exhibit other pharmacological features such as HIV-1 reverse transcriptase inhibition,[7] and blood platelet aggregation,[8] as a selective thromboxane synthetase, and anti-hypertensiveness[9,10] and antimicrobial activities.[11,12] Indeed, pyridazino[4,5-*b*]indoles are considered as aza-heterocycle alkaloids of both the β-carboline and γ-carboline scaffolds,[8–10] which exhibit cytotoxic, mutagenic, and genotoxic activities with high binding affinity to DNA.[13]

Several examples based on the carbazole scaffold show pharmacological features such as the SSR180575 analogue derived from pyridazino[4,5-*b*]indole, which showed highly potency and was a specific ligand for the PBR or TSPO receptor with high binding affinity ($K_d = 1.95 \pm 0.22$ and 4.58 ± 0.83 nM, respectively).[14,15] Harmane is a β-carboline alkaloid, which has been discovered to be an anti-tumor agent with high binding affinity to DNA and works as a Topo I inhibitor.[16] Mahanine is another example derived from the carbazole scaffold, which is utilized for the treatment of breast cancer and subtype cell lines *via* the activation of caspases and AKT deactivation.[17,18] Additionally, ellipticine is considered to be a potent antineoplastic agent,[19] as shown in Fig. 1.

Based on the above findings and in continuation of our research on the discovery and development of novel anti-cancer leads,[20–22] the present study, we established new pyridazino[4,5-*b*]indole derivatives and evaluated them against a breast cancer cell line (*in vitro*, *in vivo* and *in silico*). Two hits showed potent inhibition activity against phosphatidylinositol 3-kinase. These leads are expected to be future drugs and efficient for further investigations.

[a]*Chemistry Department, Faculty of Science, Arish University, Al-Arish 45511, Egypt. E-mail: ahmed_sarhan252@yahoo.com*

[b]*Chemistry Department, Faculty of Science, Suez Canal University, Ismailia 41522, Egypt. E-mail: Mohamed_nafie@science.suez.edu.eg; ahmed_tawfeek83@yahoo.com*

[c]*Chemistry Department, College of Science, King Saud University, P.O. Box 2455, Riyadh 11451, Saudi Arabia. E-mail: ambarakat@ksu.edu.sa*

[d]*Chemistry Department, Faculty of Science, Alexandria University, P.O. Box 426, Ibrahimia, Alexandria 21321, Egypt*

† Electronic supplementary information (ESI) available. See DOI: 10.1039/d0ra02798g

‡ M. S. N. carried out the experimental and discussion of all the biological assays.

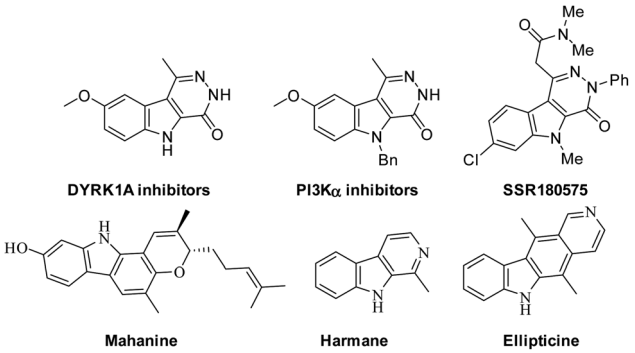

Fig. 1 Bioactive compounds containing indole with other rings.

2. Results and discussion

2.1. Synthesis and characterization

The reaction of ethyl 3-formyl-1*H*-indole-2-carboxylate **1** with hydrazine hydrate in ethanol *via* reflux afforded 3,5-dihydro-4*H*-pyridazino[4,5-*b*]indol-4-one **2** in good yield. The Michael addition of nucleophile **2** to acrylonitrile as the Michael acceptor in ethanol containing Et_3N yielded the Michael adduct **3** in excellent yield (Scheme 1).

Alkylation of **2** with a set of alkylating agents, namely amyl bromide, allyl bromide and benzyl bromide in the presence of K_2CO_3 in acetone afforded a mixture of two products, which were separated by column chromatography and identified to include alkylation at the indole nitrogen **4–6** and alkylation at both the indole and pyridazine nitrogens **7–9**. The bis(alkylated) products **7–9** were selectively obtained in excellent yields either from **2** or from the respective monoalkylated products **4–6** using KOH as a base in dimethyl sulfoxide as a solvent (Scheme 2).

Coupling of **2** with ethyl chloroacetate using K_2CO_3 in acetone afforded a mixture containing the monoester product **10** and the bis(ester) product **11**, while, KOH/DMSO afforded the bis(ester) **11**. Hydrazinolysis of the monoester **10** gave the monohydrazide **12**, whereas, hydrazinolysis of the bis(ester) **11** afforded the bis-hydrazide **13** (Scheme 3).

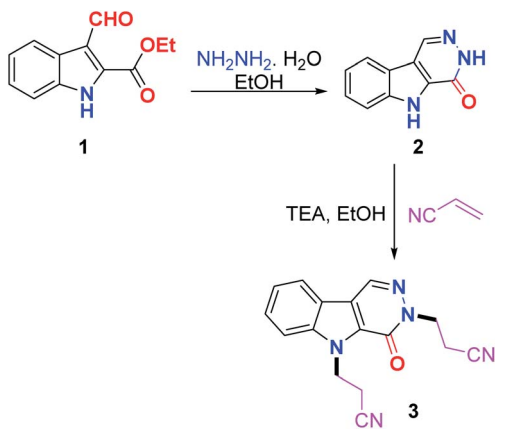

Scheme 1 Synthesis of **2** and **3**.

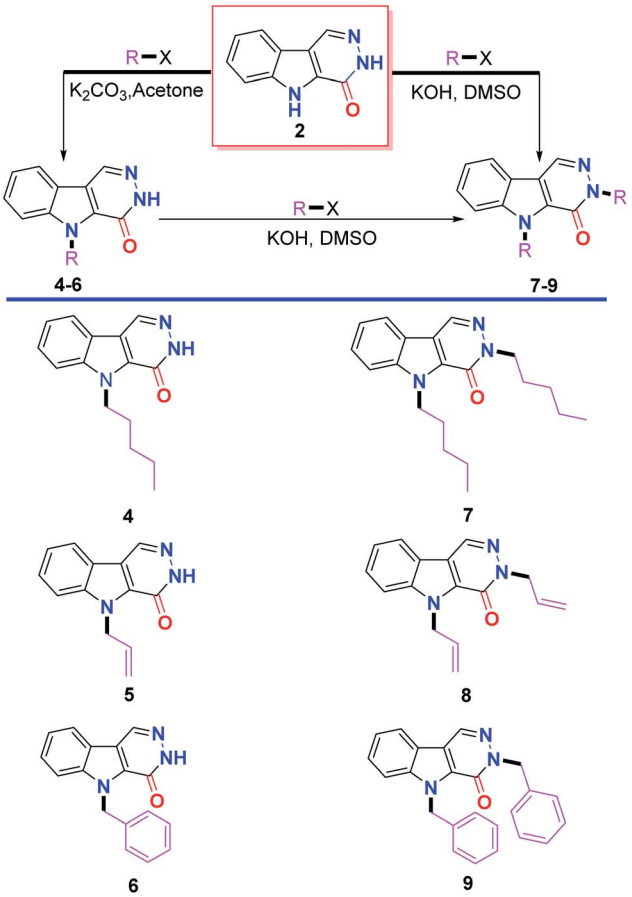

Scheme 2 Alkylation of 3,5-dihydro-4*H*-pyridazino[4,5-*b*]indol-4-one **2**.

2.2. Structural assignments

The NMR spectrum of **2** showed the four aromatic protons as two doublet of doublets and two doublets at δ 7.33, 7.51, 7.63 and 8.16 ppm. The pyridazine CH appeared as a singlet at δ 8.74 ppm, whereas, the indole and pyridazine NHs were found at δ 12.66 and 12.76 ppm, respectively. Its ^{13}C NMR spectrum displayed the pyridazine C=O at 156.19 ppm.

The NMR spectrum of the Michael adduct **3** did not show any NH signal, additionally the four methylene triplet signals appeared at δ 3.08, 3.15, 4.49 and 5.06 ppm. The methylene carbons appeared at δ 17.04, 19.39, 40.79, and 46.26 ppm, respectively, which confirm that the reaction proceed *via* aza-Michael not oxa-Michael addition.

The NMR spectra of the mono-alkylated products **4–6** and **10** showed only one NH signal at around δ 12.80 ppm, proving the alkylation of the other NH. The N-alkylation was deduced from the methylene carbon signal which was found in the ^{13}C NMR spectra of the abovementioned compounds at δ 44.74, 46.93, 47.86 and 45.99 ppm, respectively.

The dialkylated products **7–9**, and **11** did not exhibit any NH signals, which supports the dialkylation. Both alkylations were achieved by alkylation at the indole and pyridazine nitrogens. This result was obvious from ^{13}C NMR spectra, which displayed the methylene carbon signals directly attached to the indole and

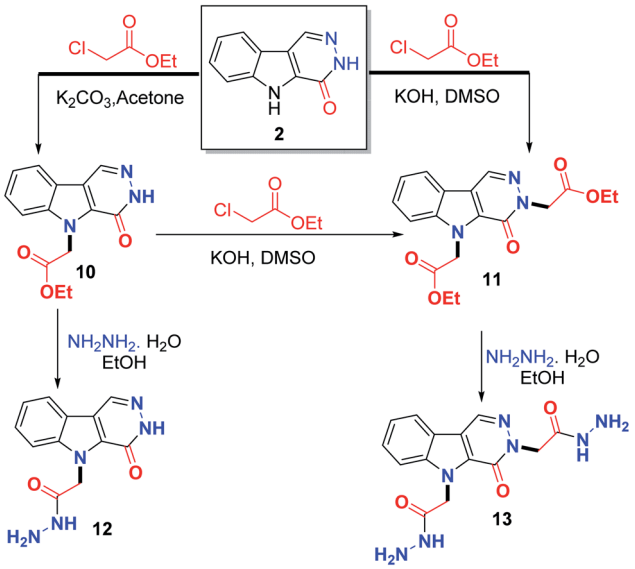

Scheme 3 Synthesis of the target hit compounds **12** and **13**.

pyridazine nitrogens at 44.70 and 50.38 ppm in **7**, δ 46.93 and 52.95 ppm in **8**, δ 47.87 and 54.04 in **9** and δ 46.47 and 52.86 ppm in **11**, respectively.

The NMR spectrum of our targeted hit **12** revealed that the hydrazide ($-CONHNH_2$) signals were D_2O exchangeable, which appeared at δ 4.26 ppm for NH_2 and 9.35 ppm for NH. The carbonyl carbon of the hydrazide group was observed at δ 167.00 ppm. The structure of the other hit molecule **13** was deduced from the exchangeable signals of the two hydrazino groups at 4.12 ppm for $2NH_2$ and δ 9.23 and 9.34 ppm for the two NH. The carbonyl carbons were detected at δ 166.96 ppm.

2.3. *In vitro* results

2.3.1. Cytotoxic screening against two cancer cell lines and normal cell line. The cytotoxic activity of the synthesized derivatives was screened against two cancer cell lines, MCF-7 and HepG2, and non-cancer cell line, GMSC, to investigate their activity and safety. The results illustrated in Table 1 reveal potential cytotoxic activity, especially for compounds **12** and **13** with IC_{50} values of 4.24 and 5.35 μM, respectively, compared to 5-FU (6.98 μM) against the MCF-7 cell line, as shown in Fig. 2. Some derivatives, including **2**, **10** and **11** showed moderate activity with IC_{50} values of 9.43, 12.4, and 9.07 μM, respectively. On the other hand, the tested derivatives showed a weak to moderate cytotoxic effect against the HepG2 cell line. In the trial to investigate the safety of the treatment with the tested compounds, they were found to be non-toxic against the normal cell line GMSC with non-detectable or high IC_{50} values. The structure–activity relationship of the potent hits **12** and **13** is attributed to the presence of the hydrazide group attached to pyridazino[4,5-*b*]indol-4-one, which provides hydrogen bond acceptors and hydrogen bond donors that best fit with the molecular targets, and thus this type of hit is expected to act as an interesting pharmacophore for anti-tumor activity.

Table 1 Cytotoxic activity against MCF-7 and HepG2 cancer cell lines and a normal cell line[a]

	IC_{50} (μM)		
Compound	MCF-7	HepG2	GMSC
2	9.43	22.78	ND
3	ND	>50	ND
5	>50	>50	>50
6	29.51	ND	>50
8	16.99	ND	ND
9	>50	ND	ND
10	12.4	36.67	>50
11	9.07	18.76	>50
12	4.25	12.75	>50
13	5.35	ND	>50
5-FU	6.98	ND	>50

[a] ND = not determined.

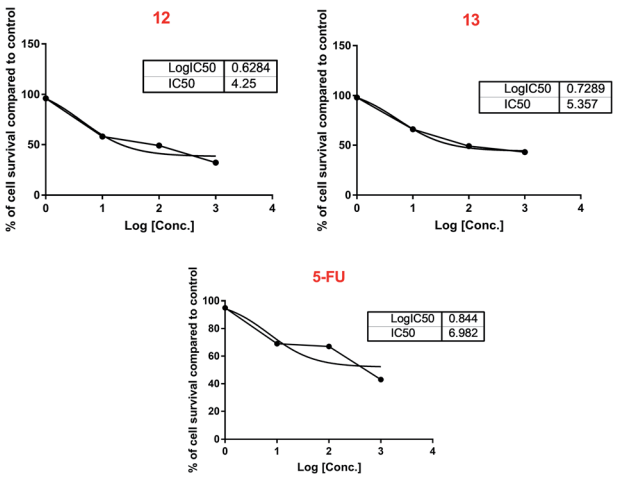

Fig. 2 Sigmoidal IC_{50} calculation curve for the most promising derivatives against the MCF-7 cell line.

2.3.2. RT-PCR results. Compound **12** was found to be the most active member in this series with an IC_{50} value of 4.25 μM against the MCF-7 breast cancer cell line. To control the apoptosis, both the intrinsic and extrinsic genes were investigated by gene expression analysis. The following genes including pro-apoptotic (P53, Bax, MDM2, and PUMA) and anti-apoptotic (Bcl-2, PI3K, AKT, and mTOR) plus β-actin, as a housekeeping gene, were collected for real-time PCR analysis. Fig. 3 illustrates that compound **12** has potential in inducing the expression of pro-apoptotic genes, such as P53, MDM2, Bax, and PUMA, with fold changes of 5.75, 6.01, 3.39, and 6.88, respectively. Moreover, it inhibited the expression of anti-apoptotic genes, such as Bcl-2, PI3K, AKT, and mTOR, with fold changes of 0.38, 0.316, 0.283, and 0.44, respectively, relative to β-actin (fold change = 1) as a house-keeping gene. Thus, the up-regulation of pro-apoptotic genes and down-regulation of anti-apoptotic genes by compound **12** relative to the control indicate its induction of apoptosis through the inhibition of the PI3K/AKT/mTOR pathway in the treated breast cancer cells.

Previous results demonstrated that 5*H*-pyridazino[4,5-*b*]indoles exhibit promising and significant anti-proliferative effects in various cell types through the PI3K/AKT/mTOR pathway.[6]

The *in silico* study indicated that compound **12** could bind efficiently with the 1e7v protein, representing the PI3K/mTOR targets. Validation of this binding was assessed on the gene expression level through the down-regulation of PI3K, AKT and mTOR.

Besides down-regulation of the PI3K/AKT/mTOR pathway, this was further validated by the activation of both extrinsic and intrinsic pathways, as a set of P53 and BAX genes, which were significantly up-regulated, while the down-regulation of the anti-apoptotic gene BCL-2 gene is in agreement with the report by Khodair *et al.*, 2019.[23] Therefore, inhibition of the PI3K/AKT/mTOR pathway resulted in the mediation of apoptosis. Our idea of using the gene expression level for elucidating the PI3K/AKT/mTOR pathway agrees with the previous study Kattan *et al.*, 2020,[24] which linked the gene expression to the inhibition of the PI3K/AKT/mTOR pathway and apoptosis.

2.4. *In vivo* results

In vivo experiments were performed to test the activity of compound **12** against EAC-bearing mice, which were divided into three groups, EAC-bearing mice as the positive control, compound **12**-treated, and 5-FU-treated EAC-bearing mice. For the analysis of the measured parameters, the survival analysis and anti-cancer efficacy of the ascetic peritoneal fluid of the mice at the end of the experiment duration (day 18) are discussed similarly as in the report by El Gohary *et al.*[25]

Treatment with compound **12** significantly increased the mean survival time (MST) to 17.2 days compared to 10 days in the EAC control, increased the life span (ILS%) by 72% and the mean survival ratio to (T/C%) 172% compared to the EAC control group. The 5-FU treatment group showed an increase in the survival parameters to 16.6 days, 66%, and 166%, respectively, as shown in Fig. 4A. Additionally, treatment with compound **12** inhibited the increase in body weight (IBW%) to 19.27% relative to the untreated EAC control values. An increase in life span is an essential criterion for anti-cancer efficiency and is directly related to a decrease in the number of viable cells and the accumulation of ascetic fluid.

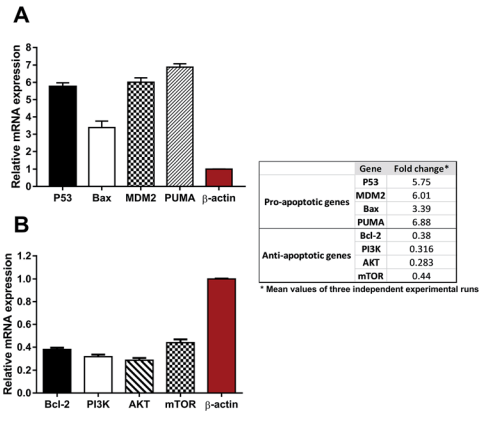

	Gene	Fold change*
Pro-apoptotic genes	P53	5.75
	MDM2	6.01
	Bax	3.39
	PUMA	6.88
Anti-apoptotic genes	Bcl-2	0.38
	PI3K	0.316
	AKT	0.283
	mTOR	0.44

* Mean values of three independent experimental runs

Fig. 3 RT-PCR analysis of (A) pro-apoptotic genes (P53, Bax, MDM2, and PUMA) and (B) anti-apoptotic genes (Bcl-2, PI3K, AKT, and mTOR) was performed after the MCF-7 cells were treated with compound **12** (5 μM) for 48 h. Red column represents that of the house-keeping gene (Fold change = 1).

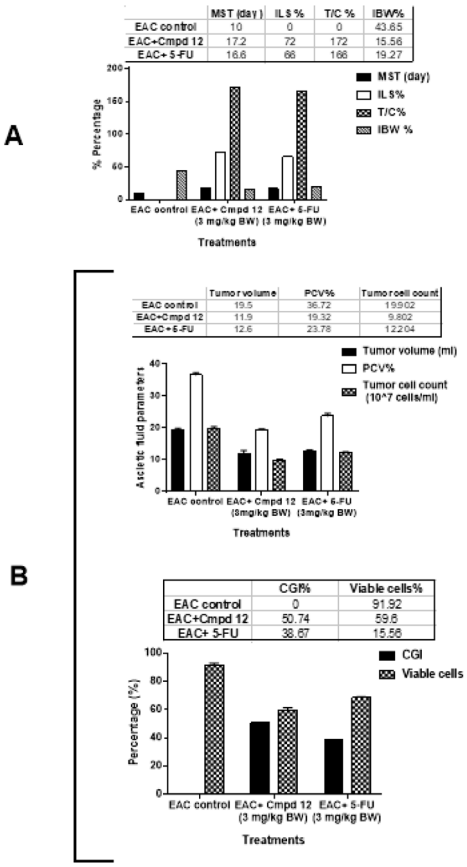

	MST (day)	ILS %	T/C %	IBW%
EAC control	10	0	0	43.65
EAC+Cmpd 12	17.2	72	172	15.56
EAC+ 5-FU	16.6	66	166	19.27

	Tumor volume	PCV%	Tumor cell count
EAC control	19.5	36.72	19.902
EAC+Cmpd 12	11.9	19.32	9.802
EAC+ 5-FU	12.6	23.78	12.204

	CGI%	Viable cells%
EAC control	0	91.92
EAC+Cmpd 12	50.74	59.6
EAC+ 5-FU	38.67	15.56

Fig. 4 *In vivo* anti-tumor activity in **12**-treated EAC-bearing mice. (A) Survival parameters, including mean survival time (MST), percentage increase in life span (ILS%), percentage MST ratio (T/C%), and percentage increase in body weight (IBW%). (B) Anti-tumor potential against ascetic fluid, including tumor volume, tumor cell count, packed cell volume (PCV%), percentage of viable cells, and cell growth inhibition (CGI%).

Fig. 4B shows the effects of compound **12** and 5-FU treatments on the ascetic peritoneal fluid of the EAC-bearing mice. Compound **12** treatment significantly decreased the tumor volume from 19.5 to 11.9 mL, packed cell volume (PCV%) from 36.72% to 19.32%, total tumor cell count from 19.9 to 9.8 $\times$ 10^7 cells per mL, percentage of viable cells from 91.9% to 59.6%, and body weight from 43.65% to 15.56% relative to the untreated EAC control. Accordingly, the percentage growth inhibition (CGI%) of compound **12** significantly increased to 50.74%, proving that its anti-cancer effectiveness is superior to that of 5-FU. Treatment with 5-FU decreased the tumor volume to 12.6 mL, packed cell volume (PCV%) to 23.78%, total tumor cell count to 12.2 $\times$ 10^7 cells per mL, and percentage of viable cells to 68.46%. Accordingly, its percentage growth inhibition (CGI%) significantly increased to 38.67%. The decrease in the parameters of ascetic peritoneal fluid may be due to the anti-proliferative action against EAC cells. The *in vivo* results

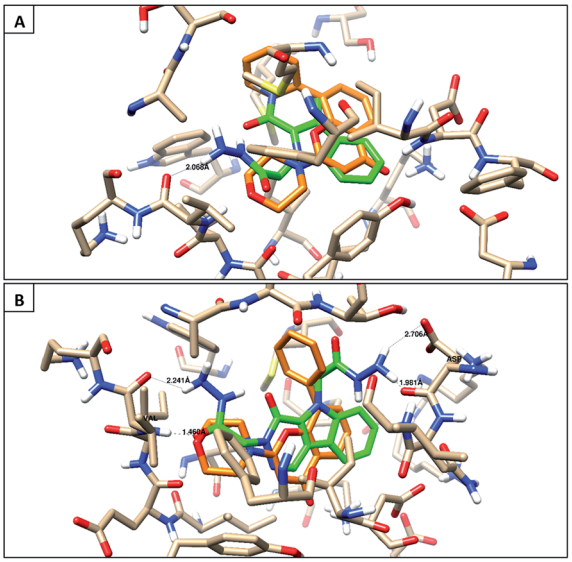

Fig. 5 Binding disposition and ligand–receptor interactions of the co-crystallized ligand (orange) and docked compounds (green). (A) compound **12** and (B) compound **13**.

followed the same trend for the elucidation of the anti-cancer activity as that by Medhat *et al.*, 2017.[26]

According to the *in vivo* results, hit **12** exhibited better activity than 5-FU, which in accordance with the *in vitro* results.

2.5. *In Silico* study

The synthesized compounds were docked for their binding affinities towards phosphoinositide 3-kinase inhibition (PDB: 1e7v) as a molecular target.[27] According to the *in silico* results, the following molecules, **2**, **10**, **11**, **12**, and **13**, have similar interaction inside the pocket matching with the co-crystallized ligand *via* the amino acid Val882, with good binding energies (−10.6 to −18.87 kcal mol^{-1}) and also exhibit good lipophilic interaction inside the pocket of the target protein with Ile 881, Val 882, Met 953, Ile 879, Met 804, Trp 812, Phe 961 and Ile 963, as illustrated in the 2D images in Table 1, ESI.† The other derivatives did not show this type of interaction with this receptor binding site. Therefore, the molecular docking study demonstrates the same perspective as the RT-PCR results to give an overview for the mode of action of compound **12** against MCF-7 cells, which may be due to the inhibition of the PI3K/AKT/mTOR pathway (Fig. 5).

3. Experimental

General: all general information about the apparatus used to confirm the chemical structure assignment can be found in the ESI.†

3.1. Synthesis of the target compounds

3.1.1. Synthesis of 3,5-dihydro-4*H*-pyridazino[4,5-*b*]indol-4-one 2. A mixture of **1** (1.0 mmol) and $NH_2NH_2 \cdot H_2O$ (2.0 mmol) was refluxed in 5 mL ethanol for 3 h, and left to cool, and the formed crystals were collected by filtration and recrystallized from ethanol.

3.1.2. 3,5-Dihydro-4*H*-pyridazino[4,5-*b*]indol-4-one 2. Yield: 75%, mp 322–323 °C [Lit. 324–326 °C [10]]. ^{1}H NMR (400 MHz, DMSO-d_6) δ 7.33 (dd, 1H, J 7.2, 7.6 Hz), 7.53 (dd, 1H, J 7.2, 8.0 Hz), 7.63 (d, 1H, J 8.4 Hz), 8.16 (d, 1H, J 8.0 Hz), 8.74 (s, 1H, CH), 12.66 (s, H, NH), 12.76 (s, H, NH); ^{13}C NMR (100 MHz, DMSO-d_6): δ 113.45, 117.98, 121.26, 121.79, 121.89, 127.44, 132.14, 133.78, 139.39, 156.19; CHN analysis calc. for $C_{10}H_7N_3O$ [185.0]: C, 64.86; H, 3.81; N, 22.69 found: C, 64.66; H, 3.91; N, 22.55.

3.1.3. Synthesis of 3,3′-(4-oxo-3*H*-pyridazino[4,5-*b*]indole-3,5(4*H*)-diyl)dipropanenitrile 3. A mixture of **2** (1.0 mmol) and acrylonitrile (2.2 mmol) in 10 mL ethanol containing Et_3N (3 mmol) was refluxed for 4 h, and left to cool at room temperature, and the precipitate was collected by filtration, dried and recrystallized from ethanol. Yield: 89%, mp 197–198 °C. ^{1}H NMR (400 MHz, DMSO-d_6) δ 3.08 (t, 2H, J 6.4 Hz, CH_2), 3.15 (t, 2H, J 6.4 Hz, CH_2), 4.49 (t, 2H, J 6.4 Hz, CH_2), 5.06 (t, 2H, J 6.4 Hz, CH_2), 7.42 (dd, 1H, J 7.2, 8.0 Hz), 7.62 (dd, 1H, J 7.2, 8.4 Hz), 7.94 (d, 1H, J 8.4 Hz), 8.21 (d, 1H, J 8.0 Hz), 8.85 (s, 1H, CH); ^{13}C NMR (100 MHz, DMSO-d_6): δ 17.04 (CH_2), 19.39 (CH_2), 40.79 (NCH_2), 46.26 (NCH_2), 112.03, 118.29, 118.73, 118.92, 120.38, 122.05, 122.76, 128.05, 129.89, 133.72, 140.04, 155.12; CHN analysis calc. for $C_{16}H_{13}N_5O$ [291.1]: C, 65.97; H, 4.50; N, 24.04 found: C, 66.01; H, 4.44; N, 23.99.

3.2. General procedure for the alkylation

3.2.1. Method A. A mixture of **2** (1.0 mmol) and K_2CO_3 (2.2 mmol) in a mixture of acetone/DMF (10: 2 mL) was stirred at room temperature for 1 h, then the appropriate alkyl halide (2.2 mmol) was added dropwise, and stirring was continued overnight. Then the solvent was evaporated under vacuum, water was added, and the precipitate was filtered. The product was purified *via* column chromatography using silica and 2 : 8 EA/*n*-hexane.

3.2.2. Method B. A mixture of **2** (1.0 mmol) and KOH (2.2 mmol) in 10 mL DMSO was stirred at room temperature for 1 h, and then the appropriate alkyl halide (2.2 mmol) was added dropwise, and subsequently stirred overnight (monitored by TLC until all **2** was converted to the dialkylated product). Then water was added, the precipitate was filtered and the products were purified either by recrystallization from ethanol or column chromatography using silica and 2 : 8 EA/*n*-hexane.

3.2.3. 5-Pentyl-3,5-dihydro-4*H*-pyridazino[4,5-*b*]indol-4-one 4. Yield: $44\%_{\text{Method A}}$, mp 161–162 °C. ^{1}H NMR (400 MHz, DMSO-d_6) δ 0.82 (t, 3H, J 7.2 Hz, CH_3), 1.23–1.32 (m, 4H, 2 CH_2), 1.77–1.84 (m, 2H, CH_2), 4.80 (t, 2H, J 7.2 Hz, NCH_2), 7.37 (dd, 1H, $J \approx$ 7.6 Hz), 7.58 (dd, 1H, J 8.0, 7.6 Hz), 7.79 (d, 1H, J 8.4 Hz), 8.20 (d, 1H, J 8.0 Hz), 8.74 (s, 1H), 12.72 (s, 1H, NH); ^{13}C NMR (100 MHz, DMSO-d_6): δ 14.19 (CH_3), 18.79 (CH_2), 22.20 (CH_2), 28.60 (CH_2), 30.38 (CH_2), 44.74 (NCH_2), 111.84, 117.84, 120.59, 122.01, 127.56, 130.54, 133.58, 139.75, 156.46; CHN analysis calc. for $C_{15}H_{17}N_3O$ [255.1]: C, 70.56; H, 6.71; N, 16.46 found: C, 70.44; H, 6.73; N, 16.33.

3.2.4. 5-Allyl-3,5-dihydro-4*H*-pyridazino[4,5-*b*]indol-4-one 5. Yield: 35%$_{\text{Method A}}$, mp 237–238 °C. ^{1}H NMR (400 MHz, DMSO-d_6) δ 4.92 (dd, 1H, J_{trans} 17.1, 1.4 Hz, H_{trans}), 5.12 (dd, 1H, J_{cis} 10.3, 1.3 Hz, H_{cis}), 5.48 (d, 2H, J 5.2 Hz, NCH_2), 6.02–6.08 (m, 1H, –C*H*=CH_2), 7.38 (dd, 1H, J 7.3, 7.6 Hz), 7.58 (dd, 1H, J 8.1, 8.2 Hz), 7.79 (d, 1H, J 8.4 Hz), 8.22 (d, 1H, J 8.0 Hz), 8.78 (s, 1H), 12.83 (s, 1H, NH); ^{13}C NMR (100 MHz, DMSO-d_6): δ 46.93 (NCH_2), 112.14, 117.04, 117.97, 120.61, 122.08, 122.26, 127.66, 130.29, 133.74, 134.50, 139.70, 156.49; CHN analysis calc. for $C_{13}H_{11}N_3O$ [225.1]: C, 69.32; H, 4.92; N, 18.66 found: C, 69.21; H, 4.79; N, 18.59.

3.2.5. 5-Benzyl-3,5-dihydro-4*H*-pyridazino[4,5-*b*]indol-4-one 6. Yield: 51%$_{\text{Method A}}$, mp 231–232 °C. ^{1}H NMR (400 MHz, DMSO-d_6) δ 6.10 (s, 2H, NCH_2), 7.37–7.30 (m, 5H), 7.37 (dd, 1H, J 7.6, 7.4 Hz), 7.54 (dd, 1H, $J \approx$ 7.7 Hz), 7.75 (d, 1H, J 8.40 Hz), 8.23 (d, 1H, J 8.0 Hz), 8.82 (s, 1H), 12.92 (s, 1H, NH); ^{13}C NMR (150 MHz, DMSO-d_6): δ 47.86 (NCH_2), 112.33, 118.16, 120.81, 122.17, 122.39, 127.58, 127.80, 127.89, 129.07, 130.34, 133.86, 138.19, 139.69, 156.70; CHN analysis calc. for $C_{17}H_{13}N_3O$ [275.1]: C, 74.17; H, 4.76; N, 15.26 found: C, 74.20; H, 4.86; N, 15.24.

3.2.6. 3,5-Dipentyl-3,5-dihydro-4*H*-pyridazino[4,5-*b*]indol-4-one 7. Yield: 29% $_{\text{Method A}}$, 71%$_{\text{Method B}}$, oil. ^{1}H NMR (400 MHz, DMSO-d_6) δ 0.82 (t, 3H, J 6.8 Hz, CH_3), 0.87 (t, 3H, J 6.8 Hz, CH_3), 1.24–1.37 (m, 8H, 4 CH_2), 1.78–1.81 (m, 2H, CH_2), 4.22 (t, 2H, J 7.2 Hz, NCH_2), 4.82 (t, 2H, J 7.2 Hz, NCH_2), 7.38 (dd, 1H, J 7.2, 7.6 Hz), 7.58 (dd, 1H, J 7.2, 8.0 Hz), 7.79 (d, 1H, J 8.4 Hz), 8.20 (d, 1H, J 8.0 Hz), 8.76 (s, 1H); ^{13}C NMR (100 MHz, DMSO-d_6): δ 14.22 (CH_3), 22.20 (CH_3), 28.47 (CH_2), 28.61 (CH_2), 28.74 (CH_2), 30.41 (CH_2), 44.70 (NCH_2), 50.38 (NCH_2), 111.88, 117.42, 120.36, 121.95, 122.14, 127.59, 130.54, 130.23, 132.92, 140.05, 155.10; CHN analysis calc. for $C_{20}H_{27}N_3O$ [325.2]: C, 73.81; H, 8.36; N, 12.91 found: C, 73.91; H, 8.31; N, 12.90.

3.2.7. 3,5-Diallyl-3,5-dihydro-4*H*-pyridazino[4,5-*b*]indol-4-one 8. Yield: 33% $_{\text{Method A}}$, 69%$_{\text{Method B}}$, oil. ^{1}H NMR (600 MHz, DMSO-d_6) δ 4.83 (d, 2H, J 5.5 Hz, NCH_2), 4.93 (d, 1H, J_{trans} 17.1, H_{trans}), 5.11 (d, 1H, J_{cis} 10.1 Hz, H_{cis}), 5.13 (d, 1H, J_{trans} 17.0 Hz, H_{trans}), 5.19 (d, 1H, J_{cis} 10.3 Hz, H_{cis}), 5.50 (d, 2H, J 5.0 Hz, NCH_2), 6.01–6.07 (m, 2H, 2 –C*H*=CH_2), 7.40 (dd, 1H, J 7.3, 7.7 Hz), 7.59 (dd, 1H, J 8.2, 7.2 Hz), 7.73 (d, 1H, J 8.4 Hz), 8.23 (d, 1H, J 7.9 Hz), 8.82 (s, 1H); ^{13}C NMR (150 MHz, DMSO-d_6): δ 46.93 (NCH_2), 52.95 (NCH_2), 112.21, 117.08, 117.66, 117.71, 120.40, 122.08, 122.43, 127.78, 129.96, 133.41, 133.83, 134.47, 140.03, 154.91; CHN analysis calc. for $C_{16}H_{15}N_3O$ [265.1]: C, 72.43; H, 5.70; N, 15.84 found: C, 72.46; H, 5.84; N, 15.93.

3.2.8. 3,5-Dibenzyl-3,5-dihydro-4*H*-pyridazino[4,5-*b*]indol-4-one 9. Yield: 41%$_{\text{Method A}}$, 86%$_{\text{Method B}}$ mp 147–148 °C. ^{1}H NMR (400 MHz, DMSO-d_6) δ 5.45 (s, 2H, NCH_2), 6.10 (s, 2H, NCH_2), 7.22–7.40 (m, 11H), 7.55 (m, 1H), 7.76 (d, 1H, J 8.5 Hz), 8.23 (d, 1H, J 8.0 Hz), 8.88 (s, 1H); ^{13}C NMR (100 MHz, DMSO-d_6): δ 47.87 (NCH_2), 54.04 (NCH_2), 112.04, 117.99, 120.57, 122.15, 122.62, 127.47, 127.84, 127.99, 128.15, 128.19, 128.93, 129.07, 129.10, 130.08, 133.69, 138.03, 138.12, 140.07, 155.38; CHN analysis calc. for $C_{24}H_{19}N_3O$ [365.1] C, 78.88; H, 5.24; N, 11.50 found: C, 78.99; H, 5.44; N, 11.44.

3.2.9. Ethyl 2-(4-oxo-3,4-dihydro-5*H*-pyridazino[4,5-*b*]indol-5-yl)acetate 10. Yield: 48%$_{\text{Method A}}$, mp 255–256 °C. ^{1}H NMR (600 MHz, DMSO-d_6) δ 1.22 (t, 3H, J 7.0 Hz, CH_3) 4.17 (q, 2H, J 7.0 Hz, CH_2), 5.68 (s, 2H, NCH_2), 7.41 (dd, 1H, J 7.4, 7.6 Hz), 7.58 (dd, 1H, J 7.6, 7.9 Hz), 7.80 (d, 1H, J 8.40 Hz), 8.23 (d, 1H, J 7.9 Hz), 8.81 (s, 1H), 12.87 (s, 1H, NH); ^{13}C NMR (150 MHz, DMSO-d_6): δ 14.1 (CH_3), 45.99 (NCH_2), 61.57 (OCH_2), 111.97, 121.88, 127.23, 127.80, 132.49, 133.17, 140.47, 148.48, 168.61 (C=O); CHN analysis calc. for $C_{14}H_{13}N_3O_3$ [271.1] C, 61.99; H, 4.83; N, 15.49 found: C, 62.03; H, 4.86; N, 15.48.

3.2.10. Diethyl 2,2′-(4-oxo-3*H*-pyridazino[4,5-*b*]indole-3,5(4*H*)-diyl)diacetate 11. Yield: 38%$_{\text{Method A}}$, 75%$_{\text{Method B}}$, mp 153–154 °C. ^{1}H NMR (400 MHz, DMSO-d_6) δ 1.18–1.22 (m, 6H, 2 CH_3) 4.12–4.19 (m, 4H, 2 CH_2), 4.99 (s, 2H, NCH_2), 5.66 (s, 2H, NCH_2), 7.43 (dd, 1H, J 7.4, 7.6 Hz), 7.61 (dd, 1H, J 7.2, 8.3 Hz), 7.81 (d, 1H, J 8.4 Hz), 8.25 (d, 1H, J 7.8 Hz), 8.87 (s, 1H); ^{13}C NMR (100 MHz, DMSO-d_6): δ 14.44, 14.47 (2 CH_3), 46.47 (NCH_2), 52.86 (NCH_2), 61.51 (OCH_2), 61.68 (OCH_2), 111.89, 118.34, 120.28, 122.14, 122.81, 128.16, 130.18, 133.81, 140.67, 155.38, 168.41 (C=O), 168.83 (C=O); CHN analysis calc. for $C_{18}H_{19}N_3O_5$ [357.1] C, 60.50; H, 5.36; N, 11.76 found: C, 60.64; H, 5.37; N, 11.73.

3.3. General procedures for hydrazinolysis

To the selected ester **10** or **11** in 10 mL ethanol, hydrazine hydrate (2.0 $mmol_{10}$ or 4.0 $mmol_{11}$) was added and refluxed for 2 h until all the esters were consumed (reaction completion was monitored by TLC), and then the reaction mixture was left to cool, and the formed precipitate was filtered, dried and recrystallized from ethanol.

3.3.1. 2-(4-Oxo-3,4-dihydro-5*H*-pyridazino[4,5-*b*]indol-5-yl) acetohydrazide 12. Yield: 91%, mp 280$_{\text{decomp.}}$ °C. ^{1}H NMR (400 MHz, DMSO-d_6) δ 4.26 (brs, 2H, NH_2, D_2O exchangeable), 5.49 (s, 2H, NCH_2), 7.37–7.63 (m, 3H), 8.21 (d, 1H, J 7.6 Hz), 8.77 (s, 1H), 9.35 (brs, 1H, NH, D_2O exchangeable), 12.76 (s, 1H, NH, D_2O exchangeable); ^{13}C NMR (100 MHz, DMSO-d_6): δ 14.1 (CH_3), 46.20 (NCH_2), 111.80, 118.07, 120.69, 121.96, 122.28, 127.61, 131.12, 133.76, 140.52, 156.71, 167.00 (C=O); CHN analysis calc. for $C_{12}H_{11}N_5O_2$ [257.1] C, 56.03; H, 4.31; N, 27.22 found: C, 56.11; H, 4.31; N, 27.12.

3.3.2. 2,2′-(4-Oxo-3*H*-pyridazino[4,5-*b*]indole-3,5(4*H*)-diyl) di(acetohydrazide) 13. Yield: 89%, mp 293–294 °C. ^{1}H NMR (400 MHz, DMSO-d_6) δ 4.26 (brs, 4H, 2 NH_2, D_2O exchangeable), 4.79 (s, 2H, NCH_2), 5.81 (s, 2H, NCH_2), 7.39–7.65 (m, 3H), 8.22 (d, 1H, J 8 Hz), 8.79 (s, 1H), 9.23 (brs, 1H, NH, D_2O exchangeable), 9.34 (brs, 1H, NH, D_2O exchangeable); ^{13}C NMR (100 MHz, DMSO-d_6): δ 46.17 (NCH_2), 52.36 (NCH_2), 111.95, 117.97, 120.49, 121.93, 122.46, 127.72, 130.69, 133.39, 140.82, 155.55, 166.96 (2C=O); CHN analysis calc. for $C_{14}H_{15}N_7O_3$ [329.1] C, 51.06; H, 4.59; N, 29.77 found: C, 51.13; H, 4.55; N, 29.76.

3.4. Biological evaluation

The cytotoxic screening using the MTT assay,[28,29] and RT-PCR[23] are provided in the ESI.†

3.5. In vivo protocol

All mice were purchased from the Laboratory of the Faculty of Veterinary Medicine, Suez Canal University. The EAC cells were purchased from the National Cancer Institute, Cairo, Egypt. In our protocol, we used a safe concentration of DMSO (5 μL/25 g for each mouse), and the treated doses were freshly prepared.

The *in vivo* experiment regarding the implantation of Ehrlich Ascites Carcinoma (EAC), experiment design, and the measurement of the parameters in this study were performed according to Nafie *et al.*, 2020.[30] and Salem *et al.*, 2016.[31] (see ESI†). All animal procedures were performed in accordance with the Guidelines for the Care and Use of Laboratory Animals of Suez Canal University and approved by the Animal Ethics Committee of the Faculty of Science. From day zero of the experiment, the mortality and body weight of the mice were monitored daily for the survival analysis (mean survival time (MST), percentage of MST ratio (T/C%), percentage increase in life span (ILS%), and increase in body weight (IBW%)). At the end of the experiment, on day 18, the mice were anesthetized and sacrificed to determine the anti-cancer potentiality of the compounds (tumor volume, packed cell volume (PCV%), tumor cell count, trypan blue exclusion assay,[32] and percentage cell growth inhibition (CGI%)).

3.6. In silico

All parameters and software used for the molecular docking study are provided in the ESI.†[26,32–34]

4. Conclusions

In summary, a series of new mono and dialkylated pyridazino [4,5-*b*]indol-4-ones **4–10** were synthesized. All the alkylation reactions were found to proceed *via* N-alkylation. Hydrazinolysis of the mono and di-esters **10** and **11** afforded the target hits mono- and bis-hydrazides **12** and **13**, respectively. The hit compound **12** exhibited interesting PI3K inhibition activity, as supported by the *in vitro*, *in vivo* and *in silico* results.

Conflicts of interest

The authors declare no conflict of interest.

Acknowledgements

The authors would like to extend their sincere appreciation to the Researchers Supporting project number (RSP-2019/64), King Saud University, Riyadh, Saudi Arabia.

References

1 M. Sriram, J. J. Hall, N. C. Grohmann, T. E. Strecker, T. Wootton, A. Franken, M. L. Trawick and K. G. Pinney, *Bioorg. Med. Chem.*, 2008, **16**, 8161–8171.
2 A. Akinleye, P. Avvaru, M. Furqan, Y. Song and D. Liu, *J. Hematol. Oncol.*, 2013, **6**, 88.
3 J. C. Chamcheu, T. Roy, M. B. Uddin, S. Banang-Mbeumi, R.-C. N. Chamcheu, A. L. Walker, Y.-Y. Liu and S. Huang, *Cells*, 2019, **8**, 803.
4 C. Porta, C. Paglino and A. Mosca, *Front. Oncol.*, 2014, **4**, 64.
5 A. Bruel, R. Bénéteau, M. Chabanne, O. Lozach, R. Le Guevel, M. Ravache, H. Bénédetti, L. Meijer, C. Logé and J.-M. Robert, *Bioorg. Med. Chem. Lett.*, 2014, **24**, 5037.
6 A. Bruel, C. Logé, M. L. de Tauzia, M. Ravache, R. Le Guevel, C. Guillouzo, J.-F. Lohier, J. S. Oliveira Santos, O. Lozach, L. Meijer, S. Ruchaud, H. Bénédetti and J.-M. Robert, *Eur. J. Med. Chem.*, 2012, **57**, 225.
7 M. Font, A. Monge, A. Cuartero, A. Elorriaga, J. J. MartinezIrujo, E. Alberdi, E. Santiago, I. Prieto, J. J. Lasarte, P. Sarobe and F. Borras, *Drug Des. Discovery*, 1997, **14**, 305.
8 A. Monge, M. I. Aldana, T. Alvarez, M. Font, E. Santiago, J. A. Latre, M. J. Bermejillo and M. J. Lopez-Unzu, *J. Med. Chem.*, 1991, **34**, 3023.
9 A. Monge, P. Parrado, M. Font and E. Fernandezalvarez, *J. Med. Chem.*, 1987, **30**, 1029.
10 A. El-Gendy and H. El-Banna, *Arch. Pharmacal Res.*, 2001, **24**, 21.
11 I. Avan, A. Guven and K. Guven, *Turk. J. Chem.*, 2013, **37**, 271.
12 A. El-Gendy, M. M. Said, N. Ghareb, Y. M. Mostafa and E. S. H. El Ashry, *Arch. Pharm.*, 2008, **341**, 294.
13 J. Chen, X. Dong, T. Liu, J. Lou, C. Jiang, W. Huang, Q. He, B. Yang and Y. Hu, *Bioorg. Med. Chem.*, 2009, **17**, 3324.
14 V. Vin, N. Leducq, F. Bono and J. M. Herbert, *Biochem. Biophys. Res. Commun.*, 2003, **310**, 785.
15 V. Papadopoulos, M. Baraldi, T. R. Guilarte, T. B. Knudsen, J. J. Lacapère, P. Lindemann, M. D. Norenberg, D. Nutt, A. Weizman, M.-R. Zhang and M. Gavish, *Trends Pharmacol. Sci.*, 2006, **27**, 402.
16 R. Cao, W. Peng, H. Chen, Y. Ma, X. Liu, X. Hou, H. Guan and A. Xu, *Biochem. Biophys. Res. Comm.*, 2005, **338**, 1557.
17 M. Das, R. Kandimalla, B. Gogoi, K. N. Dutta, P. Choudhury, R. Devi, P. P. Dutta, N. C. Talukdar and S. K. Samanta, *Pharmacol. Res.*, 2019, **146**, 104330.
18 S. Sinha, B. C. Pal, S. Jagadeesh, P. P. Banerjee, A. Bandyopadhaya and S. Bhattacharya, *Prostate*, 2006, **66**, 1257.
19 M. Stiborová, J. Poljaková, E. Martínková, L. Bořek-Dohalská, T. Eckschlager, R. Kizek and E. Frei, *Interdiscip. Toxicol.*, 2011, **4**, 98.
20 A. T. A. Boraei, M. S. Gomaa, E. S. H. El Ashry and A. Duerkop, *Eur. J. Med. Chem.*, 2017, **125**, 360.
21 A. T. A. Boraei, H. A. Ghabbour, M. S. Gomaa, E. S. H. El Ashry and A. Barakat, *Molecules*, 2019, **24**, 4471.
22 A. T. A. Boraei, P. K. Singh, M. Sechi and S. Satta, *Eur. J. Med. Chem.*, 2019, **182**, 111621.
23 A. I. Khodair, M. A. Alsafi and M. S. Nafie, *Carbohydr. Res.*, 2019, **486**, 107832.
24 S. W. Kattan, M. S. Nafie, G. A. Elmgeed, W. Alelwani, M. Badar and M. A. Tantawy, *J. Steroid Biochem. Mol. Biol.*, 2020, 105604.
25 N. S. El-Gohary, M. T. Gabr and M. I. Shaaban, *Bioorg. Chem.*, 2019, **89**, 102976.

26 D. Medhat, J. Hussein, M. E. El-Naggar, M. F. Attia, M. Anwar, Y. A. Latif, H. F. Booles, S. Morsy, A. R. Farrag, W. K. B. Khalil and Z. El-Khayat, *Biomed. Pharmacother.*, 2017, **91**, 1006.
27 E. H. Walker, M. E. Pacold, O. Perisic, L. Stephens, P. T. Hawkins, M. P. Wymann and R. L. Williams, *Mol. Cell*, 2000, **6**, 909–919.
28 T. Mosmann, *J. Immunol. Methods*, 1983, **65**, 55–63.
29 R. I. Freshney, *Culture of animal cells: a manual of basic technique and specialized applications*, Wiley-Blackwell, Hoboken, N.J., 2010.
30 M. S. Nafie, N. K. Arafa, N. K. Sedky, A. A. Alakhdar and R. K. Arafa, *Chem.-Biol. Interact.*, 2020, **324**, 109087.
31 M. L. Salem, N. M. Shoukry, W. K. Teleb, M. M. Abdel-Daim and M. A. Abdel-Rahman, *SpringerPlus*, 2016, **5**, 570.
32 W. Strober, *Curr. Protoc. Immunol.*, 2001, A.3B.1–A.3B.2.
33 D. C. Young, *Computational Drug Design*, John Wiley & Sons, Inc., Hoboken, NJ, USA, 2009.
34 M. S. Nafie, M. A. Tantawy and G. A. Elmgeed, *Steroids*, 2019, **152**, 108485.